Improved Differentiation of hESC-derived Pancreatic Progenitors by Using Human Fetal Pancreatic Mesenchymal Cells in a Micro-Scalable Three-dimensional Co-culture System

Zahra Ghezelayagh
Royan Institute for Stem Cell Biology and Technology
Mahsa Zabihi
Royan Institute for Stem Cell Biology and Technology
Ibrahim Zarkesh
Royan Institute for Stem Cell Biology and Technology
Carla A. C. Gonçalves
University of Copenhagen Faculty of Health Sciences: Kobenhavns Universitet Sundhedsvidenskabelige Fakultet
Michael Larsen
University of Copenhagen Faculty of Health Sciences: Kobenhavns Universitet Sundhedsvidenskabelige Fakultet
Newsha Hagh-parast
Royan Institute for Stem Cell Biology and Technology
Mohammad Pakzad
Royan Institute for Stem Cell Biology and Technology
Masoud Vosough
Royan Institute for Stem Cell Biology and Technology
Babak Arjmand
Tehran University of Medical Sciences
Hossein Baharvand
Royan Institute for Stem Cell Biology and Technology
Bagher Larijani
Tehran University of Medical Sciences
Anne Grapin-Botton
University of Copenhagen Faculty of Health Sciences: Kobenhavns Universitet Sundhedsvidenskabelige Fakultet
Hamid Reza Aghayan
Tehran University of Medical Sciences
Yaser Tahamtani (yasertahamtani@gmail.com)

Royan Institute for Stem Cell Biology and Technology https://orcid.org/0000-0003-2360-4985

Research Article

Keywords: AggreWell, Co-culture, Fetal mesenchyme, Niche-specific, Pancreas, Spheroid

Posted Date: June 2nd, 2021

DOI: https://doi.org/10.21203/rs.3.rs-560164/v1

Version of Record: A version of this preprint was published at Stem Cell Reviews and Reports on September 29th, 2021. See the published version at https://doi.org/10.1007/s12015-021-10266-z.

Abstract

Mesenchymal cells of diverse origins differ in gene and protein expression besides producing varying effects on their organ-matched epithelial cells' maintenance and differentiation capacity. Co-culture with rodent's tissue-specific pancreatic mesenchyme accelerates proliferation, self-renewal, and differentiation of pancreatic epithelial progenitors. Therefore, in our study, the impact of three-dimensional (3D) co-culture of human fetal pancreatic-derived mesenchymal cells (hFP-MCs) with human embryonic stem cell-derived pancreatic progenitors (hESC-PPs) development towards endocrine and beta cells was assessed. Besides, the ability to maintain scalable cultures combining hFP-MCs and hESC-PPs was investigated. hFP-MCs expressed many markers in common with bone marrow-derived mesenchymal stem cells (BM-MSCs). However, they showed higher expression of DESMIN compared to BM-MSCs. After co-culture of hESC-PPs with hFP-MCs, the pancreatic progenitor (PP) spheroids generated in Matrigel had higher expression of *NGN3* and *INSULIN* than BM-MSCs co-culture group, which shows an inductive impact of pancreatic mesenchyme on hESC-PPs beta-cells maturation. Pancreatic aggregates generated by forced aggregation through scalable AggreWell system showed similar features compared to the spheroids. These aggregates, a combination of hFP-MCs and hESC-PPs can be applied as an appropriate tool for assessing endocrine-niche interactions and developmental processes by mimicking the pancreatic tissue.

Introduction

Knowledge on normal pancreas development [1,2] and findings on *in-vitro* differentiation [3] and co-culture studies [4,5] can help us develop novel cell- and micro-tissue-based therapeutic/modeling approaches for pancreatic degenerative diseases. Human pluripotent stem cells (hPSCs), due to their unlimited proliferation capacity and their potential for differentiation into all tissues, can be used to generate pancreatic cells *in-vitro* [6]. Recapitulating signaling mechanisms involved in different stages of pancreas development has led to the development of multistep protocols to direct hPSCs differentiation to β-cells [7,8,3]. However, the insulin-producing cells differentiated in the early two-dimensional (2D) culture systems were more similar to fetal than adult β-cells [9,10]. These protocols have been continuously improved, including three-dimensional (3D) culture, but the glucose-responsiveness and functionality of adult β-cells are still challenging to reach [10-12]. Current protocols attempt to improve this by clustering endocrine cells [13] or applying metabolic stimuli [14]. Also, pancreas development is affected by extrinsic stimuli and paracrine signals of different cell types in the milieu, providing cues for organogenesis; therefore, more attention should be paid to interactions between the pancreatic epithelium and its surrounding niche cells, notably the mesenchyme, for the *in-vitro* reconstruction of pancreatic cells [15,10].

In the early stages of pancreas organogenesis, the mesenchyme envelopes the developing epithelium and establishes the most considerable portion of this niche [16,1,17]. The surrounding mesenchyme aids progenitor's expansion and, subsequently, endocrine delamination and differentiation [18,19]. Therefore, *in-vivo* cellular complexity and extrinsic signaling of the surrounding mesenchyme are essential aspects

of pancreatic tissue development. Embryonic pancreatic mesenchyme presents a different profile of genes/proteins expression and signaling pathway factors than its epithelium and even other mesenchymal sources [20-22]. Furthermore, each tissue-specific mesenchyme has unique characteristics that make it a suitable niche for proper epithelium development [23,24]. Characterization of human pancreatic-derived mesenchymal cells provided foundational insight into its unique proteome and secretome compared to bone marrow-derived mesenchymal stem cells (BM-MSCs), revealing functional properties of this native source that can be applied in diabetes regenerative medicine studies [20,24]. Transplantation of pancreatic explants, genetic manipulation, and co-culture experiments in rodents demonstrated the importance of pancreatic mesenchyme and revealed its secreted factors and signaling pathways involved in survival [25], expansion [17,26], cyto-differentiation [27,28], and morphogenesis [17] of the pancreatic epithelium. In humans, while the presence of feeder layers of the mesenchymal cell line NIH 3T3 can promote the expansion of pancreatic progenitors produced from hESCs [29], the role of mesenchyme of pancreatic origin has only been shown on cell proliferation at the endodermal stage [4].

To gain insight into the role of the pancreatic mesenchyme in humans, we focused on 3D culture systems to mimic the conditions of *in vivo* development [30,31]. The few experiments that have focused on the impact of 3D co-culture of rodent native mesenchyme with embryonic epithelial progenitors indicate the positive impact of these co-cultures towards endocrine and β-cell differentiation [28,27]. In addition, we explored approaches enabling large-scale generation of stable and uniformly sized spheroids, which will be critical for therapeutic approaches and drug screening. Microwell-based technology has been applied to control microtissue diameter and homogeneity, higher cell density, consistent spherical shape, reproducibility, and reduced need for matrix components. Microwell system was used to enhance the expansion and differentiation of hPSC to generate scalable uniformly definitive endoderm aggregates capable of applying further pancreatic and hepatic lineage differentiation [32]. Microwell 3D culture facilitated pancreatic differentiation at the pancreatic endoderm stage to produce multicellular microtissues co-expressing PDX1 and NKX6-1 [33]. As well, several micro-well chips were developed for controlled production of aggregates from different cell types such as mouse insulinoma cell line (MIN6) [34], fibroblasts [35], mesenchyme [36], and pluripotent stem cells (PSCs) to produce uniform embryoid bodies (EB) [37]. However, the influence of 3D co-culture of human native pancreatic mesenchyme on pancreas differentiation and the possibility of this method for developing large-scale co-culture platforms has not yet been investigated.

Therefor e, in this study, hESC-derived pancreatic progenitors (hESC-PPs) were co-cultivated with human fetal pancreatic-derived mesenchymal cells (hFP-MCs), sandwiched within two layers of Matrigel. After 14 days of co-culture, improved insulin expression in generated pancreatic spheroids was observed in PPs co-cultivated with hFP-MCs, compared to PPs co-cultured with BM-MSCs. For the next step, we generated a semi-large scale co-culture system in which dual-cell pancreatic aggregates (DC-PAs) were produced using an AggreWell system in a 3D condition. This system indicated a controlled and reproducible generation of 3D pancreatic aggregated with fetal mesenchymal cells.

Materials And Methods

Human pluripotent stem cell (hPSC) culture

Human pluripotent stem cell (hPSCs) lines, Royan H5 (RH5; RRID:CVCL_9386), Royan H6 (RH6; RRID:CVCL_9387) [38] and CAG-human induced pluripotent stem cell (CAG-hiPSC) were obtained from the Royan stem cell bank, Tehran, Iran. To examine different cell seeding densities in co-culture, the huES4 PDX1-GFP cell was used [39] and expanded in DEF-CS 500 (Takara) [12], and passaged with TrypLE. Experiments with this line were conducted at DanStem and approved by De Videnskabsetiske Komiteer, Region Hovedstadenunder number H-4-2013-057. Cells obtained from the Royan stem cell bank were maintained on Matrigel (Sigma-Aldrich)-coated dishes and hPSCs' culture medium that consisted of Dulbecco's modified Eagle's medium/F12 (DMEM/F12) supplemented with 20% knockout serum replacement (KoSR), 0.1 mM non-essential amino acids (NEAA), 1% penicillin/streptomycin, 1% glutaMAX, 0.1 mM β-mercaptoethanol (all from Invitrogen), 1% insulin-transferrin-selenium (ITS, Life Technologies), and 100 ng/ml basic fibroblast growth factor (bFGF, Royan Biotech, Iran). The medium was changed every day and cells were passaged every 6-8 days by collagenase/dispase (1:2) solution [collagenase IV (0.5 mg/ml, Invitrogen): dispase (1 mg/ml, Invitrogen)] for maintenance. To induce differentiation, hPSCs were singled by trypsin-EDTA (Invitrogen), treated with 10 μM Y27632 (Sigma-Aldrich) as a ROCK inhibitor (ROCKi), and seeded at a density of 200×10^3 cells/cm^2. The differentiation process was started when cells reached 80-90% of confluence (i.e. after 24-48 h).

Generation of pancreatic progenitor cells (PPs) from hPSCs

Pancreatic progenitor cells (PPs) were differentiated from hPSCs within 14 days following a standard protocol [40] with some modifications. The designed stepwise protocol included definitive endoderm (DE), posterior foregut (PF), early PP, and PP stages, respectively. For endoderm differentiation, the hPSCs were cultured for three days in endoderm base medium containing RPMI-1640 (Invitrogen), 1% glutaMAX, 1% penicillin/streptomycin, 1% NEAA, 1% bovine serum albumin (BSA; Sigma-Aldrich), and 0.1 mM β-mercaptoethanol. In order to achieve mesendoderm on the first day of differentiation, 100 ng/ml Activin A (Sigma-Aldrich) and 2 μM Chir99021 (Stemgent) were added to the medium. To induce DE formation on days 2 and 3 of differentiation, Chir99021 was removed, and cells were induced by 100 ng/ml Activin A, 50 μg/ml ascorbic acid (AA, Sigma-Aldrich), and 5 ng/ml bFGF. Next, to achieve PPs, the differentiated endoderm cells were exposed to DMEM/F12 supplemented with 1% B27 minus vitamin A (Gibco), 1% glutaMAX, 1% penicillin/streptomycin, 1% NEAA, and 1% BSA, for 11 additional days. The base medium was supplemented with 50 ng/ml fibroblast growth factor 10 (FGF10; Royan Biotech) for 2 days, and afterward, 0.25 μM KAAD-cyclopamine (CYC, TRC), 100 nM PDBu (Tocris Biosciences), 2 μM retinoic acid (RA, Sigma-Aldrich), 200 nM LDN193189 (Stemgent), 50 ng/ml FGF10, and 50 μg/ml AA were added to the base medium on days 6 and 7 to achieve early PPs. Finally, from day 8 onwards, 50 ng/ml EGF (Sigma-Aldrich), 200 nM LDN193189, 10 mM nicotinamide, 100 nM RA, 50 ng/ml FGF10, and 50 μg/ml AA were added to the base medium. At the end of days 3 and 14 of differentiation, cells were harvested and analyzed by quantitative real time-PCR (qRT-PCR), immunostaining, and flow cytometry. To examine

different cell seeding densities in co-culture, the PPs were differentiated from huES4 PDX1-GFP cell line based on a modified published protocol [41].

Human fetal donation, pancreas retrieval, and mesenchyme isolation

Human fetal pancreatic-derived mesenchymal cells (hFP-MCs) were obtained from Endocrinology and Metabolism Research Institute, Tehran University of Medical Sciences, Tehran, Iran [42]. The human fetal pancreases were harvested from legally aborted fetuses at weeks 7-9 and 14-18 of gestation following obtaining maternal written informed consent. The ethics committee approved the use of fetal tissues for research (No. EC-00264) of the Endocrinology and Metabolism Research Institute, Tehran University of Medical Sciences, Tehran, Iran. Briefly, the donated fetuses were immersed in 5% povidone-iodine solution, followed by washes in phosphate buffered saline (PBS). Afterward, the fetal pancreas was harvested by a midline laparotomy, pulled out, and dissected from surrounding tissues. Then, the fetal pancreas was washed several times and minced into small pieces. Ultimately, short enzymatic digestion was performed using 1 mg/ml collagenase for 15 min. Digestion was stopped by cold PBS, and the vials were placed for 10 min on ice. After discarding the supernatant, the pellet containing pancreatic epithelial and mesenchymal cells was re-suspended in culture media containing Dulbecco's modified Eagle's medium/low glucose (DMEM/low glucose, Thermo Scientific, USA) and 15% fetal bovine serum (FBS, Invitrogen), and kept in a 25cm^2 flask. After 2 days, unattached tissue fragments were discarded, and fresh media was added to attach MCs. For the second pancreatic mesenchymal subculture, media was changed to DMEM-LG and 10% FBS.

For examining different cell seeding densities in co-culture, experiments were performed at DanStem with human fetal pancreases obtained from material available following elective termination of pregnancy between weeks 8 and 10 at the Departments of Gynaecology at Copenhagen University Hospital (Rigshospitalet) and Hvidovre Hospital, Denmark. The regional ethics committee approved this study (permit number H-1-2012-007), and women gave their informed written and oral consent. None of the terminations were for reasons of the pathology of pregnancy or fetal abnormality. Fetal age was determined by scanning crown-rump length and by evaluation of foot length [43].

The bone marrow mesenchymal stem cells (BM-MSCs) were obtained from the Royan stem cell bank.

Expansion and characterization of hFP-MCs and BM-MSCs

hFP-MCs from three 7-9-week post-conception (WPC) (named as MC1-3) and three 14-18 WPC (named as MC4-6) fetal samples were cultured in standard MCs culture medium that contained DMEM-LG supplemented with 10% FBS, 2 mM glutaMAX, 0.1 mM NEAAs and 1% penicillin/streptomycin. The medium was changed every two days [42]. When MCs confluence became 70-80%, cells were sub-cultured at a ratio of 1:3 by trypsin-EDTA. The hFP-MCs were passaged up to passage number 9. Based on the international society for cellular therapy's (ISCT) minimal criteria, MCs from MC4-6 subcultures 4-6 were examined for mesoderm-lineage differentiation capacity and different CD marker expression. The

expression of *DESMIN* and *VIMENTIN* genes (as mesenchyme markers) from different passages of MC1-6 was also evaluated by qRT-PCR.

hESC-PPs co-culture with hFP-MCs in a 3D culture system

To evaluate hFP-MCs effect on PPs, day-14 hESC-PPs were co-cultured with hFP-MCs or BM-MSCs (control group) on GFR-matrigel-coated 96-well plate (Corning). Here, three experimental groups were considered: 1) hESC-PPs cultured solely in Matrigel (hESC-PP), 2) hESC-PPs co-cultured with hFP-MCs (CO PP/hFP-MC), and 3) hESC-PPs co-cultivated with BM-MSCs (CO PP/BM-MSC). In this study, a 3D culture system (sandwich method) was used for co-culture where different cell densities of hESC-PPs: hFP-MCs or hESC-PPs: BM-MSCs at a ratio of 1:1, were examined. The pancreatic endoderm (PE) medium used to maintain PPs in their progenitor state contained DMEM/F12, 1% penicillin-streptomycin, 1% B27 culture supplement (Gibco), 64 ng/ml bFGF, and 10 μM Y-27632 (only on the first day) [44]. Initially, a mixture of 20 μl GFR-matrigel and PE medium (3:1 ratio) was added to each well and incubated for 15 min to solidify before cell seeding. hESC-PPs and hFP-MCs or BM-MSCs were mixed in GFR-Matrigel diluted 3:1 with PE medium and transferred onto the pre-existing solidified GFR-matrigel coated plate. Afterward, the plate was centrifuged, and 100 μl of PE medium was added to each well and kept for 14 days in culture. The medium was renewed every 3-4 days.

Agarose microwell chip preparation

Non-adherent agarose microwell chips were fabricated by mold-replication technology as previously described [45]. Briefly, AggreWell 400 plate (Stem Cell Technologies, France) was used as a template. Each well contained structured polydimethylsiloxane (PDMS) surface with a standard array of 4700 pyramidal microwells with a diameter of 400 μm. The PDMS mold was peeled off after curing of AggreWells. Then, 2 ml/well of 2% (W/V) ultrapure agarose (Invitrogen) solution was poured into standard 6-well plates, and sterilized PDMS mold was placed carefully on top of the liquid and allowed to swim up. When the mold was gently removed after agarose solidification, a mirror-inverted patterned agarose surface was observed.

Dual cell pancreatic aggregate (DC-PA) generation in 3D agarose microwell chip

For cell aggregate formation, cell suspension containing a total of 235×10^4 cells/well (at a seeding density of 500 cells/microwell) of PPs and hFP-MCs (at different ratios) was seeded on agarose microwell chips. Afterward, the plate was centrifuged for 4 min at 1200 rpm, in order to capture the cells in the microwells. Next, the plate was checked under a light microscope to confirm that the cells were distributed among the microwells; cells were then incubated in PE medium at 37°C with 5% CO_2 and 95% humidity. After 48 h incubation, DC-PAs were aspirated from the microwells and placed in 30mm ultra-low attachment plates with a density of 1500 aggregates per 10 cm^2 in the same maintenance medium used during aggregate formation. The images of DC-PAs formed were obtained daily using a digital camera to measure the diameter and number of the aggregates and were quantified by ImageJ. Aggregates size and number are reported as mean ± SEM.

Flow cytometry analysis

Flow cytometry was performed to quantify DE and PPs differentiation efficiency on days 3 and 14 of differentiation. Briefly, cells were dissociated by trypsin/EDTA for 5 min at 37˚C and washed with PBS. After centrifugation at 1500 rpm for 5 min, the cell pellet was fixed, permeabilized, and blocked. The cell pellet was re-suspended in primary antibody solution overnight, then treated with secondary antibody for 2 h at room temperature (RT). Quantification was performed by BD FACS Calibur flow cytometer (BD Biosciences), and the data were analyzed using Flowing Software (version 2.4.2). The primary and secondary antibodies used in this study are listed in Supplementary Table 1.

Immunostaining analysis

For immunocyto-staining, differentiated samples were fixed in 4% paraformaldehyde (PFA, Sigma-Aldrich) at RT for 20 min. For immunohisto-staining, co-culture and DC-PA samples were fixed in 4% paraformaldehyde at RT overnight, processed, embedded in paraffin, and sectioned at a thickness of 5 µm using a microtome (MicromHM325, Thermo Scientific). After deparaffinization and rehydration of the sections, heat-mediated antigen retrieval was performed in citrate buffer (pH 6.0, Dako) or Target Retrieval Solution High (pH 9.0, Dako) in Retriever 2100 device according to the primary antibodies data sheet instructions. Samples and slides were washed in 0.05% Tween-PBS (Sigma-Aldrich), permeabilized in 0.2% Triton X-100 (Sigma-Aldrich), blocked in 5% BSA (or 10% secondary antibody host serum) for 45-60 min and treated with primary antibodies at 4°C, overnight. Next, they were exposed to secondary antibodies at RT for 1 h in the dark. Cell nuclei were stained using 1 mg/ml 4’, 6-diamidino-2-phenylindole (DAPI, Sigma-Aldrich). The samples were observed under Olympus BX51/IX71 fluorescence microscopes equipped with an Olympus DP72 digital camera or on microscopic plates of Zeiss LSM800 confocal microscope. For quantifying protein expression efficiency in the differentiation process of RH5-ESC and CAG-hiPSC cells, seven 40X frames were randomly captured from different areas of each sample in 3 independent repeats and counted by ImageJ software. The percentages of expression were calculated according to the number of positive cells per total cells stained with DAPI. The primary and secondary antibodies used in this study are listed in Supplementary Table 1. Three slides from each sample were stained with hematoxylin and eosin (H&E) for observing morphological structures.

RNA isolation and quantitative real time- PCR (qRT-PCR)

We performed qRT-PCR for evaluating proliferation, mesenchymal and pancreatic differentiation specific genes at the transcriptional level. First, total RNA was extracted by RNeasy Micro Kit (Qiagen) based on the manufacturer’s protocol. A spectrophotometer (WPA, Biowave II) was used to evaluate RNA concentration and purity. cDNA was synthesized from 1 µg of total RNA using Takara cDNA Synthesis Kit (Takara). Quantification of the transcript was performed by Applied Bio-system (ABI, Step One Plus) using SYBR Green reagent (Applied Biosystems) and 25 ng/µl of each sample. The relative expression levels of the target genes were normalized against *GAPDH* as the housekeeping gene and calculated based on 2^-ΔΔCt and 2^-ΔCt method for differentiation process samples and co-culture/ DC-PA samples, respectively. A “control” was used to diminish or eliminate the effect of the housekeeping gene expressed

by the mesenchyme in the co-culture groups. The “control” contained a mix of hESC-PPs and hFP-MCs which each were separately kept in Matrigel along with the other groups for 14 days. At the end of the culture period, hESC-PPs and hFP-MCs were mixed together and considered as a single sample, “the hESC-PP”, for RNA extraction. The samples were collected from at least three independent biological replicates. The primer sequences are mentioned in Supplementary Table 2.

Live-dead assessment

To evaluate the viability of cells after co-culture and DC-PAs formation, live-dead assessment was performed using Fluorescein Diacetate (FDA, Sigma-Aldrich) and Propidium Iodide (PI, ThermoFisher) double staining. Here, 20 µl of FDA stock solution and 50 µl of PI stock solution were dissolved in 10 ml PBS [46]. For staining, FDA/PI solution was added directly to the culture, incubated for 5 min in the dark at RT and observed under Zeiss LSM800 confocal microscope.

hFP-MCs labeling with PKH26

For investigating the contribution and position of hFP-MCs in co-culture and in DC-PAs, hFP-MCs were labeled with the fluorescent vital dye PKH26 (Sigma-Aldrich) according to the manufacturer’s instructions. Briefly, 1 µl of PKH26 dye was diluted in 50 µl diluent C (from the manufacturer’s labeling kit) and added to 2-3×10^6 suspended hFP-MCs which were already diluted with 50 µl diluent C. Then, the suspension was incubated for 7-10 min at RT. The reaction was ended by adding 2 ml FBS, and cells were washed with DMEM/F12 to remove the excess dye. Finally, cells were observed under Zeiss LSM800 confocal microscope with an excitation wavelength of 551 nm and an emission wavelength of 567 nm.

Animals

ICR mice (*Mus musculus*) were housed at the University of Copenhagen with a standard 12 hours light/dark schedule. All experiments were performed according to ethical guidelines approved by the Danish Animal Experiments Inspectorate (Dyreforsøgstilsynet). For embryo staging, the day of vaginal plug was considered E0.5. All the embryonic stages used are stated in the main text or in the figure legends. Male and female embryos were used for all the experiments.

Statistical analysis

All data are presented as the mean ± SEM. Immunofluorescence images were quantified using ImageJ software. All statistical analyses of the data were done using Graphpad Prism 8 software by either unpaired t-test or one-way ANOVA followed by parametric and non-parametric tests. The differences among experimental groups were considered statistically significant when the p-value was less than 0.05.

Results

hPSCs express pancreatic specific markers through our differentiated protocol

During our stepwise pancreatic progenitor (PP)-directed differentiation protocol, hPSCs were induced on Matrigel through 14 days in five consecutive steps (Fig. 1a). PSCs, definitive endoderm (DE), and PP cells were evaluated on days 0, 3, and 14 of differentiation at mRNA and protein levels. Morphological assessment of RH6-ESCs showed typical characteristics of hPSCs- defined borders, large nucleus, and obvious nucleolus, which changed during differentiation (Fig. 1b and c). OCT4 and NANOG protein expression indicated initial pluripotency efficiency of RH6-ESCs in culture (Fig. 1c). Besides, DE induction was confirmed by immunostaining and flow cytometry on day 3 of differentiation with an expression of 94.7% ±2.2 and 89.2% ±8.2 positive cells for FOXA2 and SOX17 markers, respectively (Fig. 1d and e). In the next step, the expression of SOX9, PDX1, and NKX6-1 markers on day 14 post-differentiation indicated differentiation towards the PP stage (Fig. 1f). Characterization of PPs using flow cytometry also indicated 79.8% ±9.1 and 16.6% ±9.8 protein expression of PDX1, and NKX6-1 markers in RH6-ESC, respectively (Fig. 1g). qRT-PCR analysis indicated an increase in *SOX17* expression on day 3 and in *PDX1* and *NKX6-1* on day 14 compared to day 0 (Fig. 1h). Therefore, the treatment process was able to induce PPs with high efficiency from RH6-ES cell line.

To evaluate the reproducibility of our established method, we induced two other pluripotent cell lines, namely, RH5-ESC and CAG-hiPSC using this PP differentiation protocol and achieved results similar to those previously reported for RH6-ESCs at DE and PP stages (Fig. S1). To confirm the pluripotency of these cell lines, we also characterized them for OCT4 and NANOG expression at protein level (Fig. S1c and d). In RH5-ESC and CAG-hiESC cell lines, approximately 85% and 79% of cells were positive for FOXA2 marker, and approximately 81% and 77% were positive for SOX17, respectively on day 3 of differentiation (Fig. 1Se and f). Characterization of PPs on day 14 indicated that approximately 78% and 71% of cells were positive for PDX1, and approximately 12% and 16% were positive for NKX6-1, respectively, in RH5-ESC and CAG-hiESC cell lines (Fig. 1Sg and h).

Isolated hFP-MCs demonstrate classical MSC-like phenotype in culture

hFP-MCs were isolated and expanded from six different human fetus samples in different gestational weeks (Fig. 2a) [42]. To determine mesenchymal markers, which were specifically expressed in the mesenchymal compartment of the human pancreas but not in the epithelium, immunostaining on early and late human fetal pancreas samples and also on E14.5 mouse samples was performed. The results showed VIMENTIN and DESMIN expression, two previously reported pan-mesenchymal markers [47-50], in the MCs that surround the epithelium. Desmin was expressed in MCs of E14.5 mouse pancreas but not in its epithelium (Fig S2a). At 8 WPC, 94.4% ± 2.13 of the MCs expressed VIMENTIN, and approximately 88% ± 4.2 expressed DESMIN (Fig. 2b), suggesting that a large subset of the cells but not all co-expressed the two markers. Vimentin was also detected at weeks 14-16 in most MCs (Fig. S2b). Then, hFP-MCs were cultured in adherent conditions and expanded for forthcoming co-culture experiments and were compared to BM-MSC for phenotypic, functional, and molecular characteristics under identical growth conditions. Bright-field images of hFP-MC1 (passage 3) and hFP-MC4 (passage 4) demonstrated a dynamic spindle-shaped and fibroblast-like cell morphology as observed for BM-MSCs (Fig. 2c). The morphology of other pancreatic mesenchymal samples from passages 1-7 was also similar to BM-MSCs

(Fig. S2c). VIMENTIN was expressed at a very high level in hFP-MCs from all stages as well as BM-MSC, during culture (Fig 2d). Immunostaining for DESMIN indicated different expression profiles in hFP-MC samples (Fig. 2d and S2d and e). These results were confirmed at the mRNA level, showing a significantly higher expression for hFP-MCs than BM-MSCs (Fig. 2e). Also, the expression of *DESMIN* in the lines derived from 7-9 WPC fetuses (hFP-MC1 and hFP-MC2) was significantly higher compared to those derived from 14-18 WPC fetuses (hFP-MC5 and hFP-MC6) (Fig. 2e and S2f). Though the human fetal pancreas is not expected to give rise to bones, adipose tissue or cartilage under normal developmental conditions, hFP-MCs demonstrated tri-lineage differentiation potential towards osteogenic, adipogenic and chondrogenic, lineages *in-vitro* similar to BM-MSCs, as shown by calcium deposition (Alizarin Red), lipid droplet formation (Oil Red), and glycoprotein deposition (Alcian Blue), respectively (Fig. 2f). Flow cytometry analysis demonstrated that hFP-MCs expressed classical MC surface markers, including CD73, CD90, and CD105 (Fig. 2g). Like BM-MSCs, hFP-MCs did not express hematopoietic (CD34 and CD45) and HLA-DR markers (Fig. 2h). Overall, the results confirmed that hFP-MCs have many typical characteristics of MSCs.

hFP-MCs upregulate *INSULIN* expression in co-cultivated hPSC-PPs

To investigate the effect of hFP-MCs on proliferation and further differentiation of hESC-PPs in 3D, a co-culture system embedded in Matrigel was applied (Fig. 3a) [51,44]. Different initial cell seeding densities were tested to achieve an optimal and suitable concentration for the co-culture procedure. An optimal ratio (1:1) and initial cell density (2000 cells/well for each cell type) was selected for further experiments based on the morphology of the formation of 3D epithelial structures, cell density avoiding overcrowding, and expression of PP and endocrine markers. This experimental group showed and maintained a high expression of PDX1-GFP and higher levels of endocrine markers compared to 1000 (of each cell type) cells/well group (Fig. S3). In all three experimental groups (i.e., hESC-PP, CO PP/hFP-MC, and CO PP/BM-MSC), PP spheroids were generated after 14 days of culture (Fig. 3b). In the CO PP/hFP-MC and CO PP/BM-MSC groups, MCs were stretched in the Matrigel in a 3D formation surrounding the pancreatic spheroids. The MCs did not compact around the spheroids and only made loose contact around the formed spheroids (Fig. 3b and c). The dense or hollow spherical epithelial structures of the spheroids and the scattered mesenchyme around them in Matrigel were also observed in H&E staining (Fig. 3c). hFP-MCs labeled with the general membrane marker PKH26 indicated the presence of hFP-MCs after 48 h culture (Fig. 3d). For all three groups, live/dead staining revealed high viability of spheroids and mesenchyme cells after 14 days of co-culture (Fig. 3e).

The epithelial structure of the formed spheroids was confirmed after 14 days of co-culture by their expression of E-CADHERIN (Fig. 4a). The mesenchymal marker, VIMENTIN, was expressed in co-cultured groups around the formed spheroids, while in some samples, their extensions to some extent penetrated into the organoids (Fig. 4b). SOX9 protein was detected in the three mentioned groups showing the progenitor state. INSULIN positive cells were observed in spheroids of both CO PP/BM-MSC and CO PP/hFP-MC groups (Fig. 4c). In order to evaluate the difference of the proliferation rate between the experimental groups, *Ki67* gene expression was analyzed, indicating no significant difference between

the groups (Fig. 4d). Although the expression of PP genes (*PDX1* and *NKX6-1*), endocrine progenitor gene (*NGN3*), and beta and alpha genes (*INSULIN* and *GLUCAGON*) was higher in the CO PP/hFP-MC group, this increase was only significant for *NGN3* and *INSULIN* genes, compared to the CO PP/BM-MSC group (P= 0.01 and 0.036, respectively) (Fig. 4e). As it was shown (Fig. 2) that *DESMIN* had a higher expression in hFP-MCs, gene expression analysis of co-cultures also indicated a significant enrichment for this gene in the CO PP/hFP-MC group compared to other experimental groups (P= 0.009) (Fig. 4e). Altogether, the obtained results demonstrate that hFP-MC can improve maturation of hESC-PP towards endocrine lineage and insulin-producing cells compared to CO PP/BM-MSCs.

Towards scalable production of dual cell- pancreatic aggregate (DC-PA)

To move a step forward and overcome the limitations regarding our protocol, such as low scalability and Matrigel disadvantages, a 3D non-adherent micro-mold technology was used. DC-PAs were generated by mixing hESC-PPs and hFP-MCs in 3D agarose microwell chips (Fig. 5a). Initially, hESC-PPs were co-cultivated with hFP-MCs at different ratios of 1:1, 2:1 and 5:1 in microwell chips. The bright-field images clearly showed the gathering of hESC-PPs/hFP-MCs in the center of each microwell after forced cell aggregation (Fig. 5b), which was followed by the formation of stable cell aggregates after incubating the microwell plate for 48 h (Fig. 5c). Following harvesting and counting, each well contained 3375 ±209.7 DC-Pas, which were transferred into a static suspension culture. For future applications such as drug screening or *in-vivo* transplantation, the formed DC-PAs must be able to maintain their size and shape under *in-vitro* conditions; therefore, they were kept in static suspension culture in PE medium. Morphologically, only at 1:1 cell ratio, uniformly-sized DC-PAs were observed (Fig. 5d) with a mean diameter of 89.94 ±1.53 µm. Cell clusters from other cell ratios (2:1 and 5:1) did not preserve a compact and spheroid-like structure in static suspension conditions (Fig. S4a). Therefore, the rest of the experiments were followed by the cell ratio 1:1. After 4 days of aggregate maintenance, a significant increase ($P < 0.0001$) in aggregates size (average diameter of aggregates 144.1 ±2.315 µm) (Fig. 5e) and a significant decrease ($P < 0.0001$) in the number of aggregates (average number of aggregates 1220 ±108.5) (Fig. 5f) were observed. hFP-MCs labeled with PKH26 indicated hFP-MCs in DC-PAs after 24 h in the microwell system and after 4 days in culture (Fig. 5g). Live/dead staining of the aggregates revealed high viability of DC-PAs during culture (Fig. 5h). Uniform spherical and dense epithelial morphological structures were observed in the DC-PAs by H&E staining (Fig. 5i). The immunostaining of SOX9 marker in DC-PAs after 4 days in culture indicated the progenitor state of the generated DC-PAs (Fig. 5j). QRT-PCR analysis revealed that PPs in the DC-PAs preserved their progenitor state after 4 days in culture than day 0 (Fig. 5k). The expression of *DESMIN* as a mesenchymal marker was also investigated (Fig. 5k), and higher expression of this marker after 4 days in culture was observed. Altogether, round-shaped and uniformly-sized DC-PAs with well-defined borders can be formed and maintained stable in culture for short periods to be considered for *in-vivo* transplantations.

To investigate whether the DC-PAs can be kept in suspension for a more extended period, the DC-PAs at 1:1 cell ratio were kept for additional 5 more days in static suspension culture (9-day culture) (Fig. S4b). There was a significant increase in aggregates diameter during the culture (Fig. S4c) with a significant

decrease in their number (Fig. S4d). Labeling hFP-MCs with PKH26 indicated the presence of hFP-MCs in DC-PAs (Fig. S4e). Live/dead staining of the aggregates revealed high viability of DC-PAs. However, a hollow spherical structure was observed in the center of the aggregates during 9 days in culture (Fig. S4f). QRT-PCR analysis revealed that although no significant differences in endocrine progenitor and endocrine genes expression in DC-PAs were observed, *PDX1* expression was significantly increased after 9 days in culture compared to day 0 (Fig. S4d).

Discussion

Over the past two decades, many efforts have been made to differentiate PSCs into insulin-secreting cells by mimicking the precise molecular course of pancreatic development. D'Amour et al. in 2006, for the first time, differentiated PPs from hESCs with an efficiency of approximately 12% of insulin-producing cells which were not glucose-responsive [7]. Also, the same group showed that after being transplanted into mice, PPs were able to complete their differentiation into pancreatic β-cells, and human Insulin was detected in mice blood [8]. Lastly, in 2014, two different groups reported production of insulin-producing cells from hESCs that were monohormonal and could restore the animal's blood sugar to normal levels much faster than previously reported after transplantation into diabetic animal models. The efficiency of $PDX1^+$ cells in both approaches was > 80%, and a variable number of 30-60% NKX6-1 cells were obtained [52,41]. Although the PPs could differentiate into insulin-producing cells using these approaches, the reproducibility of the ability to secrete Insulin in response to glucose remains unsure [53]. In the current study, the efficiency of $PDX1^+$ and $NKX6\text{-}1^+$ cells in all three cell lines was approximately 80% and 13-23%, respectively. Therefore, we claimed that we obtained PPs that can be used for co-culture in the next steps.

MSCs can be derived from various tissue sources, and it has been reported that they reflect the properties of their tissue of origin [54]. The choice of an MSC source for clinical use should reflect the extent of pluripotency balance, ease of isolation, and ethical issues related to isolation [55]. Adult MSCs are of relatively inferior quality compared to fetal stem cells in various aspects such as frequency, proliferation potential and rate, and multilineage differentiation potential, all of which decrease with increasing age [55,56]. The proliferative and differentiating capacities of fetal MSCs are higher due to their embryonic origin [57]. The bone marrow can be a difficult source of MSCs since the technique is invasive and associated with appreciable morbidity; also, the number of cells obtained can be low, and cell quality may depend on the age of the donor. Therefore, researchers have drawn attention to the use of alternative mesenchymal sources, including fetal tissues [58]. In our study, BM-MSCs were used for comparison with hFP-MCs as they are used in clinical and therapeutic approaches as a "gold standard" MSC type. *In-vitro* analysis also showed that islet-derived MSCs have similar, but not identical, phenotypic, biologic, and immunologic characteristics to BM-MSCs [59]. In this study, we provided evidence that both studied MCs are $VIMENTIN^{high}$ positive cells while DESMIN is only highly expressed in hFP-MCs, which even its expression in younger pancreas fetuses seems to be higher. However a study on *DESMIN* and *VIMENTIN* expression can be conducted on hFP-MCs from different gestational weeks and different subcultures to

gain a wider insight on hFP-MCs differences. Recently, a study demonstrated that adult pancreatic-derived MCs in comparison to BM-MSCs, represent tissue-specific MSC features with unique proteomic, secretory, and functional characteristics which are associated with endothelial cell chemotaxis, angiogenesis and islet regeneration [24]. Cooper et al. concluded that niche-specific mesenchyme or its secretome could be used for regenerative medicine applications. They also showed that the potency of pancreatic mesenchyme was quantitatively restricted when differentiated to adipose lineage [24], which was also similarly observed in our study with fetal pancreatic mesenchyme.

Studies have shown that the co-culture of PPs with non-epithelial cells or their conditioned media increases insulin-like cell formation *in-vitro*, demonstrating the importance of these cell-cell communications and their interactions during pancreatic organogenesis [54,60]. Co-culture can be a simple and effective way to enhance survival or differentiation of desired progenitors by influencing cell-cell interactions, signaling pathways, and secreted molecules in the co-culture environment [54]. Pancreatic co-culture studies were mainly conducted using rat or mouse tissues [27,28], while in our study, we showed the impact of human fetal pancreatic mesenchyme on hESC-derived PPs. Sneddon et al. co-cultured a subset of mouse/human pancreatic-derived mesenchyme samples with hESC-derived endodermal or endocrine progenitors in a 2D culture system. Though the lines showed very heterogeneous effects that could not be attributed to a specific species, age at collection or stage, they identified two mouse mesenchymal lines promoting the expansion of endoderm and two promoting the formation of more Neurog3^{+} cells, one of which from adult human islets and one from E13.5 mouse pancreatic mesenchyme. [4]. Though they showed that endocrine differentiation could be achieved after these co-cultures they did not investigate whether the efficiency of this differentiation was affected by the mesenchyme [4]. In the present study, however, further differentiation of PPs was detected in the 3D culture system, while MSCs did not affect PP spheroids proliferation rate. By labeling hFP-MCs with vital dye and VIMENTIN immunostaining, we proved the presence and contact of mesenchyme with pancreatic spheroids during co-culture. In few instances, high amounts of MCs completely surrounded the spheroids and the MC extensions entered the organoids.

Yung et al. in 2019, demonstrated that the presence of appropriate cross-talk between PPs and niche-specific mesenchyme is necessary for normal pancreatic 2D and 3D differentiation; however, even other closely related MCs such as gastrointestinal stromal cells could not achieve this aim [23]. In our study the positive impact of niche-specific mesenchyme on the increment of endocrine-specific gene expression was observed when compared to BM-MSc co-culture group or PPs group. Other studies have also indicated the impact of murine or rat pancreatic mesenchyme on the PDX1^{+} progenitor proliferation rate increment [27] and higher percentages of endocrine marker expression such as Insulin [28] when co-cultivated with their own epithelium.

Different *in-vitro* pancreatic co-culture studies with different cell ratio combinations have been conducted so far. Takebe et al. applied a ratio of 10:5:2 for Min6 cells, human umbilical vein endothelial cells (HUVECs), and BM-MSCs, respectively, and observed the generation of vascularized and complex condensates via *in-vivo* self-organization [5,61]. In a more recent study, PPs, endothelial cells, and MSCs

all derived from ESCs, were used at a ratio of 10:5:5 to generate pancreatic organoids which exhibited some functionality after transplantation in NUDE mice [62]. Both studies transplanted the multicellular organoids immediately after their formation *in-vitro*, observing the multicellular organoid functionality *in-vivo*. In our study, based on previous observations, we used the ratio of 1:1 for PPs and hFP-MCs co-culture showing an increment in beta cell-specific gene expression level after 14 days of *in-vitro* co-culture.

In several studies, Matrigel is used as a substrate for MCs migration in order to self-organize multicellular organoids containing HUVECs [5,62]. In contrast, other studies formed organoids from single-cell mouse PPs inside Matrigel forming a 3D culture system [63,64]. Sugiyama et al. indicated that pancreatic spheroids were formed inside Matrigel without the contribution of mesenchyme; however, MCs were needed for the survival of single-cell PPs in each passage. Moreover, the MCs secretion and their contact with the formed spheroids seemed to enhance PPs differentiation towards beta cells [63]. In our study, however, the spheroids were located between two layers of Matrigel instead of being inside a bubble-shaped structure [63,64], which allowed the formed structures to locate at a certain distance from the surface and the surrounding environment rather than becoming scattered throughout the matrix volume.

To further upscale our co-cultures, we used a non-adhesive agarose microwell platform as a 3D culture system for DC-PAs generation by using hESC-PPs and hFP-MCs. Using this method, approximately 3400 aggregates per well (in a 6-well plate) were produced after harvesting, and each aggregate had an average diameter of 51.37–192.4 μm. Previously, it has been shown that integration of islet cells and human amniotic epithelial cells in a 3D agarose-patterned microwell improves viability, functionality, and engraftment in generated islet organoids [65]. However, until now, controlled and reproducible generation of 3D pancreatic aggregates from pancreatic mesenchyme and PPs with optimal size has not been reported. In addition, aggregates grown in static or dynamic suspension conditions can be harvested easily without any additional forces, which prevents damage to aggregates during harvesting. Our microwell chip was made of agarose as a low-cost, accessible, re-usable, and non-adherent material to support cell assembly with the capacity to create micro-molds with various sizes and shapes, modifying the initial cell density and diameter of microwells, the size of the aggregates could be changed. Although we showed that our co-culture method is scalable, it should be mentioned here that some differences exist between the two co-culture systems used in this study. In the sandwich method, hFP-MCs are suspended within the Matrigel in which pancreatic organoids are forming, while the DC-PAs are generated by force aggregation and have the cell-cell contact of two cell types from the beginning of the culture duration. It is observed that in the sandwich method, in addition to the hFP-MCs secretions' impact, some of them have surrounded the spheroids and even penetrated inside them during the 14-day culture period, while the hFP-MCs secretion and cell-cell contact effectiveness are applied from the beginning of culture in the force aggregation method. Moreover, no ECM such as Matrigel is used in the latter.

Based on the achieved results, the co-culture of hFP-MCs with hESC-PPs produced a positive effect on further differentiation of hESC-PPs towards endocrine cells. Besides, we investigated the controlled formation of pancreatic aggregates and their morphology, viability, cell distribution, and functionality.

After keeping DC-PAs in suspension culture, they maintained their progenitor state. Identifying effective signaling pathways in this co-culture can be the next step for further research. Also, obtaining the secretomes of hESC-PPs, hFP-MCs, and the co-cultured cells, and comparing the proteins and transcripts of all three groups, may give further insights into pancreatic development processes. Large-scale production of DC-PAs, can be regarded as an appropriate tool for later studies on endocrine-niche interactions and developmental processes, as well as transplantation, and drug and genetic screening.

Declarations

Acknowledgment

We deeply thank Keiichi Katsumoto for providing us the E14.5 mouse IHF Desmin staining images. This study was funded by Royan Institute for Stem Cell Biology and Technology (RI-SCBT) and the Lotus Charity Investment Foundation, Royan Institute.

Funding: This study was funded by Royan Institute for Stem Cell Biology and Technology (RI-SCBT) and the Lotus Charity Investment Foundation, Royan Institute.

Conflicts of interest/ competing interest: The authors have no conflicts of interest.

Ethics approval: All mice experiments were performed according to ethical guidelines approved by the Danish Animal Experiments Inspectorate (Dyreforsøgstilsynet). The ethics committee of the Endocrinology and Metabolism Research Institute, Tehran University of Medical Sciences, Tehran, Iran, approved the use of fetal tissues for research (No. EC-00264). The Danmark regional ethics committee approved this study (permit number H-1-2012-007) for the use of human fetal pancreases, and women gave their informed written and oral consent.

Consent to participate: Written informed consent was obtained from women which their fetal pancreases where used.

Consent for publication: Not applicable

Availibility of data and material: All data generated or analysed during this study are included in this published article and its supplementary information file. They are also available from the corresponding author on reasonable request.

Code availibilty: Not applicable

Authors contributions: The conception and design of the study was done by [Yaser Tahamtani, Hamid Reza Aghayan, and Anne Grapin-Botton]. Material preparation, data collection and analysis were performed by [Zahra Ghezelayagh, Mahsa Zabihi, Ibrahim Zarkesh, Carla A. C. Gonçalves, Michael Larsen, Newsha Hagh-parast, and Mohammad Pakzad]. Adminestiative support was done by [Masoud Vosough, Hossein Baharvand, Babak Arjmand, and Bagher Larijani] The first draft of the manuscript was

written by [Zahra Ghezelayagh and Mahsa Zabihi], and all authors commented on previous version of the manuscript. All authors read and approved the final manuscript.

References

1. Larsen HL, Grapin-Botton A (2017) The molecular and morphogenetic basis of pancreas organogenesis. *Seminars in cell & developmental biology*, 66,51-68
2. Petersen MB, Gonçalves CA, Kim YH, Grapin-Botton A (2018) Recapitulating and deciphering human pancreas development from human pluripotent stem cells in a dish. In: Current topics in developmental biology, vol 129. Elsevier, pp 143-190
3. Rezania A, Bruin JE, Riedel MJ et al. (2012) Maturation of human embryonic stem cell-derived pancreatic progenitors into functional islets capable of treating pre-existing diabetes in mice. *Diabetes*, 61 (8),2016-2029. doi:10.2337/db11-1711
4. Sneddon JB, Borowiak M, Melton DA (2012) Self-renewal of embryonic-stem-cell-derived progenitors by organ-matched mesenchyme. *Nature*, 491 (7426),765-768
5. Takebe T, Enomura M, Yoshizawa E et al. (2015) Vascularized and complex organ buds from diverse tissues via mesenchymal cell-driven condensation. *Cell stem cell*, 16 (5),556-565
6. Babiker NE, Gassoum A, Abdelraheem NE et al. (2017) The progress of stem cells in the treatment of diabetes mellitus type 1. *Progress in Stem Cell*, 4 (01),175-188
7. D'Amour KA, Bang AG, Eliazer S et al. (2006) Production of pancreatic hormone–expressing endocrine cells from human embryonic stem cells. *Nature biotechnology*, 24 (11),1392-1401
8. Kroon E, Martinson LA, Kadoya K et al. (2008) Pancreatic endoderm derived from human embryonic stem cells generates glucose-responsive insulin-secreting cells in vivo. *Nature biotechnology*, 26 (4),443-452
9. Hrvatin S, O'Donnell CW, Deng F et al. (2014) Differentiated human stem cells resemble fetal, not adult, beta cells. *Proc natl acad sci U S A*, 111 (8),3038-3043. doi:10.1073/pnas.1400709111
10. Johnson JD (2016) The quest to make fully functional human pancreatic beta cells from embryonic stem cells: climbing a mountain in the clouds. *Diabetologia*, 59 (10),2047-2057
11. Nostro MC, Sarangi F, Yang C et al. (2015) Efficient generation of NKX6-1+ pancreatic progenitors from multiple human pluripotent stem cell lines. *Stem Cell Reports*, 4 (4),591-604. doi:10.1016/j.stemcr.2015.02.017
12. Ameri J, Borup R, Prawiro C et al. (2017) Efficient generation of glucose-responsive beta cells from isolated GP2+ human pancreatic progenitors. *Cell Reports*, 19 (1),36-49
13. Nair GG, Liu JS, Russ HA et al. (2019) Recapitulating endocrine cell clustering in culture promotes maturation of human stem-cell-derived β cells. *Nature cell biology*, 21 (2),263-274
14. Davis JC, Alves TC, Helman A et al. (2020) Glucose response by stem cell-derived β cells in vitro is inhibited by a bottleneck in glycolysis. *Cell Reports*, 31 (6),107623

15. Abdelalim EM, Emara MM (2015) Advances and challenges in the differentiation of pluripotent stem cells into pancreatic β cells. *World journal of stem cells*, 7 (1),174-181
16. Angelo JR, Tremblay KD (2018) Identification and fate mapping of the pancreatic mesenchyme. *Developmental biology*, 435 (1),15-25
17. Landsman L, Nijagal A, Whitchurch TJ et al. (2011) Pancreatic mesenchyme regulates epithelial organogenesis throughout development. *PLoS biology*, 9 (9),e1001143
18. Seymour PA, Serup P (2019) Mesodermal induction of pancreatic fate commitment. *Seminars in cell & developmental biology*, 92,77-88
19. Sakhneny L, Khalifa-Malka L, Landsman L (2019) Pancreas organogenesis: Approaches to elucidate the role of epithelial-mesenchymal interactions. *Seminars in cell & developmental biology*, 92,89-96
20. Guo T, Landsman L, Li N, Hebrok M (2013) Factors expressed by murine embryonic pancreatic mesenchyme enhance generation of insulin-producing cells from hESCs. *Diabetes*, 62 (5),1581-1592
21. Russ HA, Landsman L, Moss CL et al. (2016) Dynamic proteomic analysis of pancreatic mesenchyme reveals novel factors that enhance human embryonic stem cell to pancreatic cell differentiation. *Stem cells international*, 2016
22. Byrnes LE, Wong DM, Subramaniam M et al. (2018) Lineage dynamics of murine pancreatic development at single-cell resolution. *Nature communications*, 9 (1),1-17
23. Yung T, Poon F, Liang M et al. (2019) Sufu-and Spop-mediated downregulation of Hedgehog signaling promotes beta cell differentiation through organ-specific niche signals. *Nature communications*, 10 (1),1-17
24. Cooper TT, Sherman SE, Bell GI et al. (2020) Characterization of a Vimentin high/Nestin high proteome and tissue regenerative secretome generated by human pancreas-derived mesenchymal stromal cells. *Stem Cells*, 38 (5),666-682
25. Golosow N, Grobstein C (1962) Epitheliomesenchymal interaction in pancreatic morphogenesis. *Developmental biology*, 4 (2),242-255
26. Duvillié B, Attali M, Bounacer A et al. (2006) The mesenchyme controls the timing of pancreatic β-cell differentiation. *Diabetes*, 55 (3),582-589
27. Attali M, Stetsyuk V, Basmaciogullari A et al. (2007) Control of β-cell differentiation by the pancreatic mesenchyme. *Diabetes*, 56 (5),1248-1258
28. Scavuzzo MA, Yang D, Borowiak M (2017) Organotypic pancreatoids with native mesenchyme develop Insulin producing endocrine cells. *Scientific reports*, 7 (1),10810
29. Trott J, Tan EK, Ong S et al. (2017) Long-term culture of self-renewing pancreatic progenitors derived from human pluripotent stem cells. *Stem cell reports*, 8 (6),1675-1688
30. Clevers H (2016) Modeling development and disease with organoids. *Cell*, 165 (7),1586-1597
31. Xu H, Jiao Y, Qin S et al. (2018) Organoid technology in disease modelling, drug development, personalized treatment and regeneration medicine. *Experimental hematology oncology*, 7 (1),30

32. Ungrin MD, Clarke G, Yin T et al. (2012) Rational bioprocess design for human pluripotent stem cell expansion and endoderm differentiation based on cellular dynamics. Wiley Online Library,
33. Tran R, Moraes C, Hoesli CAJSr (2020) Controlled clustering enhances PDX1 and NKX6. 1 expression in pancreatic endoderm cells derived from pluripotent stem cells. 10 (1),1-12
34. Bernard AB, Lin C-C, Anseth KS (2012) A microwell cell culture platform for the aggregation of pancreatic β-cells. *Tissue engineering part C: Methods*, 18 (8),583-592
35. Khademhosseini A, Ferreira L, Blumling III J et al. (2006) Co-culture of human embryonic stem cells with murine embryonic fibroblasts on microwell-patterned substrates. *Biomaterials*, 27 (36),5968-5977
36. Zhao X, Qiu X, Zhang Y et al. (2016) Three-dimensional aggregates enhance the therapeutic effects of adipose mesenchymal stem cells for ischemia-reperfusion induced kidney injury in rats. *Stem cells international*, 2016
37. Antonchuk J (2013) Formation of embryoid bodies from human pluripotent stem cells using AggreWell™ plates. In: Basic Cell Culture Protocols. Springer, pp 523-533
38. Baharvand H, Ashtiani SK, Taee A et al. (2006) Generation of new human embryonic stem cell lines with diploid and triploid karyotypes. *Dev Growth Differ*, 48 (2),117-128. doi:10.1111/j.1440-169X.2006.00851.x
39. Cowan CA, Klimanskaya I, McMahon J et al. (2004) Derivation of embryonic stem-cell lines from human blastocysts. 350 (13),1353-1356
40. Lipsitz YY, Woodford C, Yin T et al. (2018) Modulating cell state to enhance suspension expansion of human pluripotent stem cells. *Proceedings of the national academy of sciences*, 115 (25),6369-6374
41. Rezania A, Bruin JE, Arora P et al. (2014) Reversal of diabetes with insulin-producing cells derived in vitro from human pluripotent stem cells. *Nat Biotechnol*, 32 (11),1121-1133. doi:10.1038/nbt.3033
42. Larijani B, Arjmand B, Ahmadbeigi N et al. (2015) A simple and cost-effective method for isolation and expansion of human fetal pancreas derived mesenchymal stem cells. *Archives of Iranian medicine*, 18 (11),770-775
43. Evtouchenko L, Studer L, Spenger C et al. (1996) A mathematical model for the estimation of human embryonic and fetal age. *Cell transplantation*, 5 (4),453-464
44. Gonçalves CA, Larsen, M., Jung, S., Stratmann, J., Nakamura, A., Leuschner, M., Hersemann, L., Keshara,R., Perlman, S., Lundvall, L., Langhoff Thuesen, L., Juul Hare, K., Amit, I., Jørgensen, A., Kim, Y.H., del Sol, A., Grapin-Botton, A. (2021) A 3D system to model human pancreas development and its reference single cell transcriptome atlas identify signaling pathways required for progenitor expansion. . *Nature Communications*, In Press
45. Dahlmann J, Kensah G, Kempf H et al. (2013) The use of agarose microwells for scalable embryoid body formation and cardiac differentiation of human and murine pluripotent stem cells. *Biomaterials*, 34 (10),2463-2471
46. Jiajia L, Shinghung M, Jiacheng Z et al. (2017) Assessment of neuronal viability using fluorescein diacetate-propidium iodide double staining in cerebellar granule neuron culture. *JoVE* (123),e55442

47. Ye L, Yu Y, Zhao Y (2020) Icariin-induced miR-875-5p attenuates epithelial-mesenchymal transition by targeting hedgehog signaling in liver fibrosis. *Journal of Gastroenterology Hepatology*, 35 (3),482-491
48. Jin J, Zhang Z, Chen J et al. (2019) Jixuepaidu Tang-1 inhibits epithelial-mesenchymal transition and alleviates renal damage in DN mice through suppressing long non-coding RNA LOC498759. *Cell Cycle*, 18 (22),3125-3136
49. Liu Y, Deng B, Zhao Y et al. (2013) Differentiated markers in undifferentiated cells: expression of smooth muscle contractile proteins in multipotent bone marrow mesenchymal stem cells. *Development, growth differentiation*, 55 (5),591-605
50. Mansuroglu T, Dudás J, Elmaouhoub A et al. (2009) Hepatoblast and mesenchymal cell-specific gene-expression in fetal rat liver and in cultured fetal rat liver cells. *Histochemistry cell biology international*, 132 (1),11
51. Greggio C, De Franceschi F, Figueiredo-Larsen M et al. (2013) Artificial three-dimensional niches deconstruct pancreas development in vitro. *Development*, 140 (21),4452-4462. doi:10.1242/dev.096628
52. Pagliuca FW, Millman JR, Gurtler M et al. (2014) Generation of functional human pancreatic beta cells in vitro. *Cell*, 159 (2),428-439. doi:10.1016/j.cell.2014.09.040
53. Takahashi Y, Takebe T, Taniguchi H (2016) Engineering pancreatic tissues from stem cells towards therapy. *Regenerative therapy*, 3,15-23
54. Li XY, Wu SY, Leung PS (2019) Human fetal bone marrow-derived mesenchymal stem cells promote the proliferation and differentiation of pancreatic progenitor cells and the engraftment function of islet-like cell clusters. *International journal of molecular sciences*, 20 (17),4083
55. Esteban-Vives R, Ziembicki J, Sun Choi M et al. (2019) Isolation and Characterization of a Human Fetal Mesenchymal Stem Cell Population: Exploring the Potential for Cell Banking in Wound Healing Therapies. *Cell transplantation*, 28 (11),1404-1419
56. Lee OK, Kuo TK, Chen W-M et al. (2004) Isolation of multipotent mesenchymal stem cells from umbilical cord blood. *Blood*, 103 (5),1669-1675
57. in't Anker PS, Scherjon SA, Kleijburg-van der Keur C et al. (2004) Isolation of mesenchymal stem cells of fetal or maternal origin from human placenta. *Stem cells*, 22 (7),1338-1345
58. Soncini M, Vertua E, Gibelli L et al. (2007) Isolation and characterization of mesenchymal cells from human fetal membranes. *Journal of tissue engineering and regenerative medicine*, 1 (4),296-305
59. Kim J, Breunig MJ, Escalante LE et al. (2012) Biologic and immunomodulatory properties of mesenchymal stromal cells derived from human pancreatic islets. *Cytotherapy*, 14 (8),925-935
60. Jaramillo M, Mathew S, Mamiya H et al. (2014) Endothelial cells mediate islet-specific maturation of human embryonic stem cell-derived pancreatic progenitor cells. *Tissue engineering part A*, 21 (1-2),14-25
61. Takahashi Y, Sekine K, Kin T et al. (2018) Self-condensation culture enables vascularization of tissue fragments for efficient therapeutic transplantation. *Cell reports*, 23 (6),1620-1629

62. Soltanian A, Ghezelayagh Z, Mazidi Z et al. (2019) Generation of functional human pancreatic organoids by transplants of embryonic stem cell derivatives in a 3D-printed tissue trapper. *Journal of cellular physiology*
63. Sugiyama T, Benitez CM, Ghodasara A et al. (2013) Reconstituting pancreas development from purified progenitor cells reveals genes essential for islet differentiation. *Proceedings of the national academy of sciences*, 110 (31),12691-12696
64. Greggio C, De Franceschi F, Figueiredo-Larsen M, Grapin-Botton A (2014) In vitro pancreas organogenesis from dispersed mouse embryonic progenitors. *JoVE* (89),e51725
65. Lebreton F, Lavallard V, Bellofatto K et al. (2019) Insulin-producing organoids engineered from islet and amniotic epithelial cells to treat diabetes. 10 (1),1-12

Figures

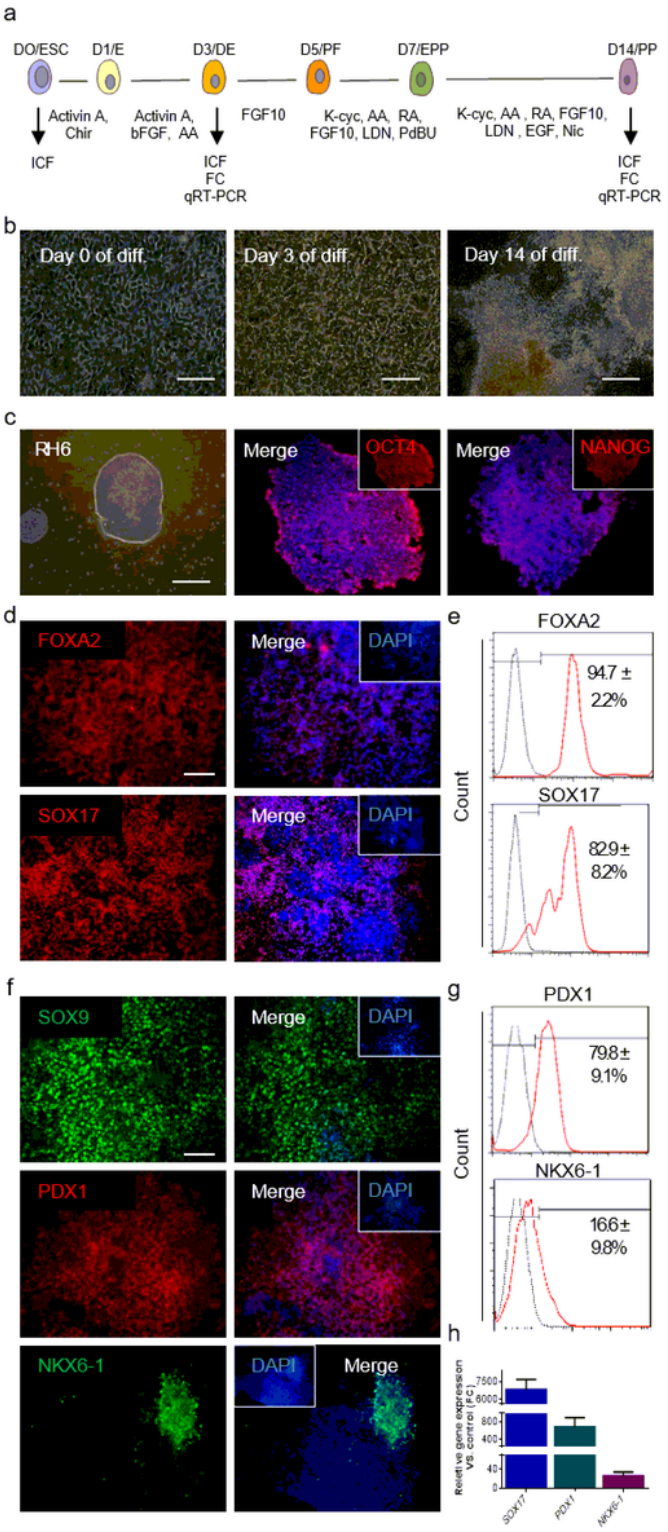

Figure 1

Stepwise differentiation of ESC towards pancreatic progenitors (PPs) a) A schematic presentation of pancreatic progenitor cells (PPs) induction from human pluripotent cells (hPSCs). Key steps and manipulations during 14 days of differentiation and evaluations of specific differentiation steps are illustrated. D, day; E, endoderm; DE, definitive endoderm; PF, posterior foregut; EPP, early pancreatic progenitor; PP, pancreatic progenitor; AA, ascorbic acid; K-cyc, KAAD cyclopamine; RA, retinoic acid; Nic,

nicotinamide; ICF, Immunocytofluorescent; FC, Flow cytometry; qRT-PCR; Quantitative Real Time-PCR. b) Bright-field images of days 0, 3, and 14 of differentiation on RH6-ESCs. Scale bars: 50, 100, and 100 μm, respectively. diff, differentiation. c) Bright-field image (Left panel) and representative immunostaining of OCT4 and NANOG pluripotency markers (Middle and Right panels, respectively) of RH6-ESCs colony on Matrigel before starting differentiation. Scale bar: 500 μm. d) Immunostaining was done on day 3 of differentiated cells for FOXA2 and SOX17 endodermal markers. Scale bar: 200 μm. e) Flow cytometry analysis of FOXA2 and SOX17 markers on day 3 of differentiation. f) Immunostaining was done on day 14 for SOX9, PDX1, and NKX6-1 PP markers. Scale bar: 100 μm. g) Flow cytometry analysis of PDX1 and NKX6-1 markers on day 14 differentiated cells. h) qRT-PCR analysis of SOX17 gene on day 3 and PDX1 and NKX6-1 genes on day 14 of differentiation. Gene expression was normalized against that of undifferentiated RH6-ESCs; n=4 biological samples, two technical repeats each. All error bars represent SEM. Nuclei are stained blue with DAPI. Bright-field and immunostaining pictures showed are representative of at least three independent experiments (n=3).

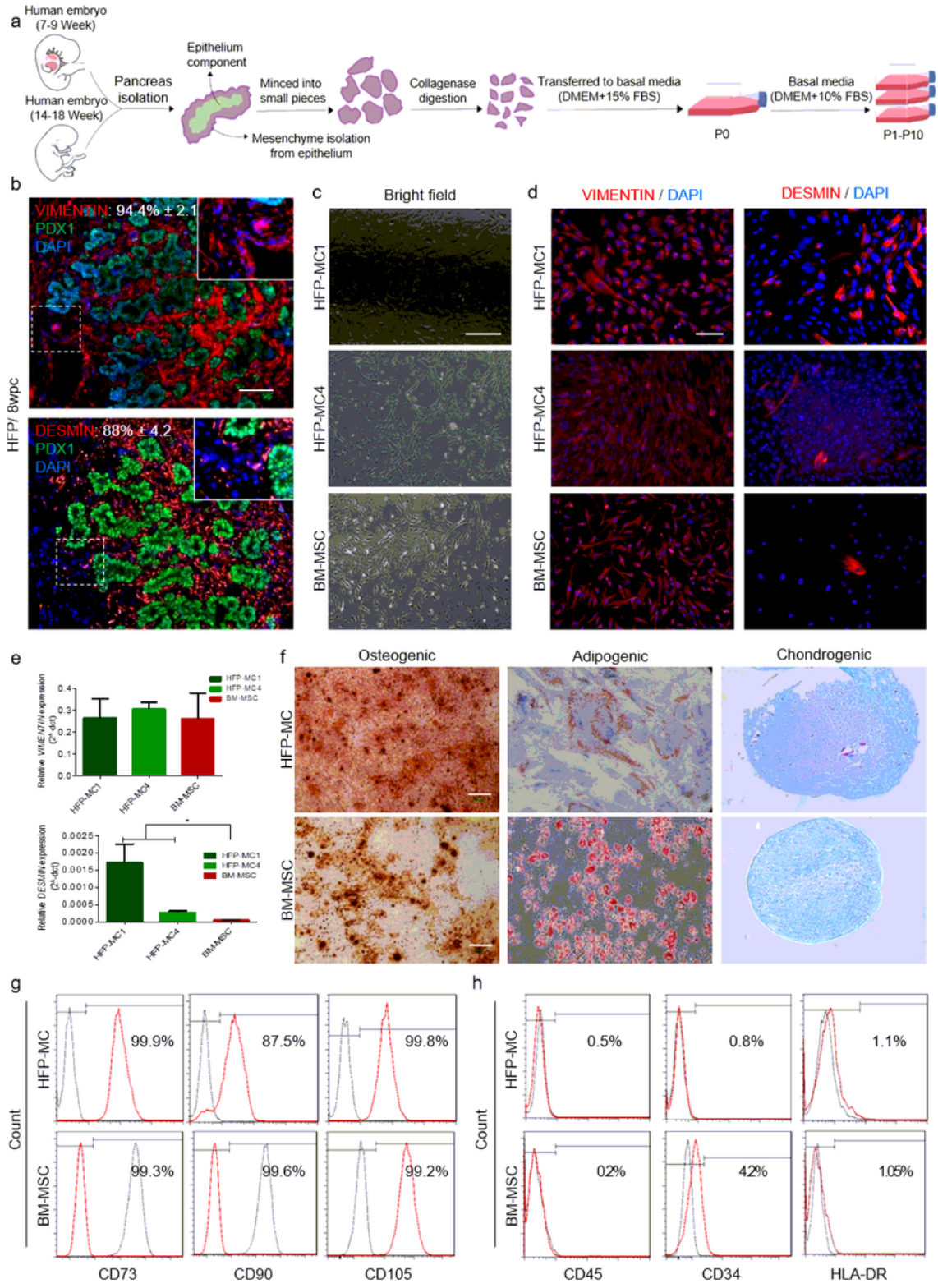

Figure 2

Human fetal pancreatic-derived mesenchymal cells (hFP-MCs) cultivation and characterization a) A schematic view of human fetal pancreatic mesenchyme isolation, expansion, and characterization. b) Immunostaining done for 8 weeks post-conception (WPC) human fetal pancreas demonstrates VIMENTIN- and DESMIN-positive mesenchymal cells (MCs) surrounding PDX1 positive epithelium cells. Scale bar: 200μm. c) Bright-field images of human fetal pancreatic-derived mesenchymal cells (hFP-MC1-

derived from a 7-week fetus and hFP-MC4–derived from a 14-week fetus) and bone marrow-mesenchymal stem cells (BM-MSC) in culture demonstrate the mesenchymal morphology of both cell types. Scale bar: 500 µm. d) Immunocytofluorescent staining indicates VIMENTIN-positive MCs for hFP-MC1 (passage 3), hFP-MC4 (passage 4) and BM-MSC during culture (Left panel). Immunocytofluorescent images for DESMIN marker indicate a higher expression of this marker in hFP-MCs compared to BM-MSC during culture (Right panel). Scale bar: 200 µm. e) Relative expression of VIMENTIN and DESMIN genes (2^-Δct) in hFP-MC1, hFP-MC4 and BM-MSC. n= 3 biological replicates. All bars represent a mean of 3 different passages (P2-8). All error bars represent SEM. f) Osteogenic, adipogenic, and chondrogenic differentiation derived from hFP-MC4 (passage 6) and BM-MSC indicate that hFP-MCs, similar to BM-MSC, have the ability to differentiate towards osteocyte, adipocyte, and chondrocyte. g) The expression of specific mesenchymal CD markers (CD73, CD90 and CD105) is demonstrated in hFP-MC4 (passage 6) and BM-MSC cells by flow cytometry analysis. h) The lack of hematopoietic markers (CD45 and CD34) and HLA-DR is demonstrated in hFP-MC4 and BM-MSC cells by flow cytometry analysis.

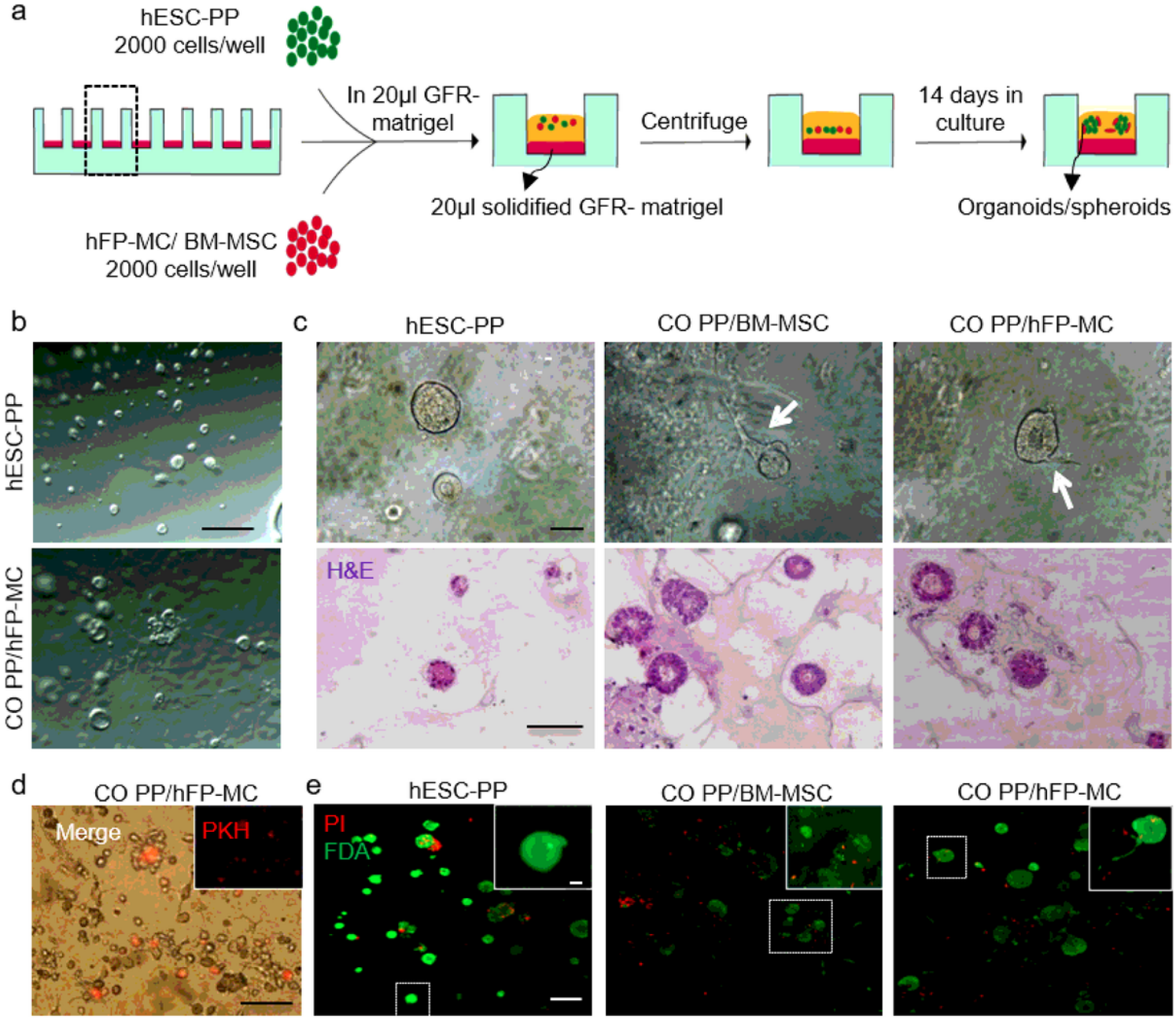

Figure 3

Generation of spheroids through 3D co-cultivation of hESC-PP and hFP-MC a) A schematic illustration of the protocol used to co-culture hESC-PP and hFP-MC or hESC-PP and BM-MSC in GFR-matrigel. 2000 cells/well of hESC-PP were co-cultured with 2000 cells/well of hFP-MC or BM-MSC (at 1:1 ratio) in 96-well plates. A 3D culture system (sandwich method) was applied for co-culture and cells were mixed in GFR-Matrigel diluted 3:1 with PE medium and placed on top of solidified GFR-matrigel. Co-culture with BM-MSC was considered the control group. hESC-PP, human embryonic stem cell-derived pancreatic progenitor cells; hFP-MC, human fetal pancreatic- mesenchymal cells; BM-MSC, Bone marrow mesenchymal stem cells; GFR-matrigel, Growth factor reduced Matrigel; PE medium, pancreatic endoderm medium. b) Microscopic images of hESC-PP co-cultured with hFP-MC (CO PP/hFP-MC) compared with hESC-PP cultured solely in Matrigel on day 14. MCs in contact with pancreatic spheroids are clearly observed in the lower image. c) Upper panel, bright field images of spheroids generated in 3 different groups (hESC-PP, CO PP/BM-MSC, and CO PP/hFP-MC) on day 10 of culture. Lower panel, hematoxylin and eosin (H&E) staining of spheroids generated in 3 mentioned groups after 14 days of culture. Scale bars: 50 μm (upper panel) and 100 μm (lower panel). d) PKH26-labeled hFP-MC after 24 hours in co-culture. Scale bars: 200 μm. e) Confocal images of live-dead staining for spheroids in the 3 groups after 14 days in 3D culture system. PI indicates dead cells while FDA indicates live cells. Scale bar: 100 μm. White boxes are higher magnifications of white dot boxes. Scale bar: 20 μm.

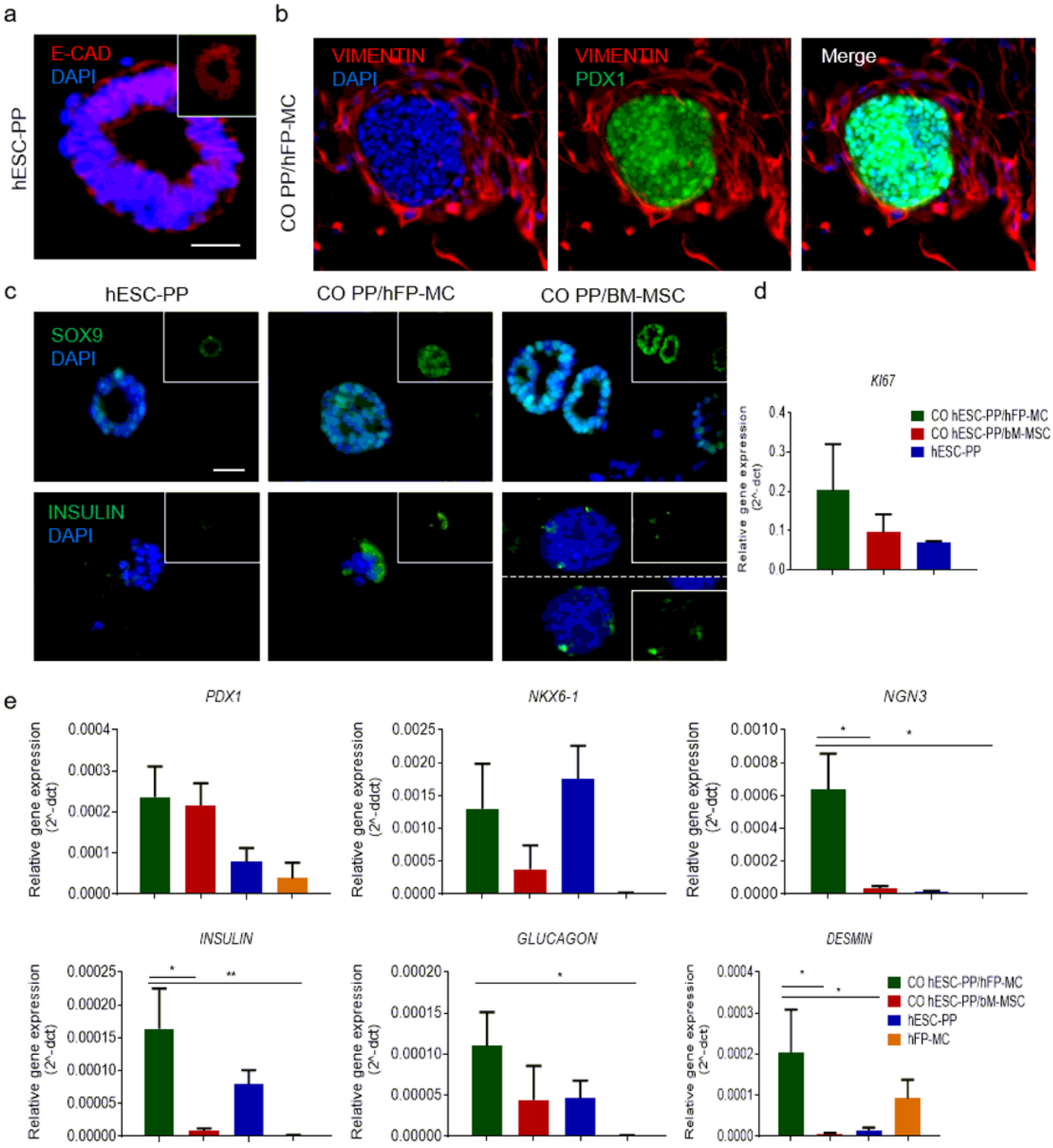

Figure 4

Maturation of hESC-PP after co-culturing with hFP-MCs a) Upper image: Immunostaining of CADHERIN epithelial marker in a typical spheroid in co-culture demonstrating its epithelial feature. Scale bar: 20 µm. Lower image: Immunostaining of VIMENTIN (mesenchymal marker) and PDX1 (pancreatic progenitor (PP) marker) proteins in CO PP/hFP-MC showing MCs surrounding the pancreatic organoid/spheroid and in contact with it. Scale bar: 10 µm. b) Immunostaining of SOX9 (PP marker) INSULIN (endocrine marker)

proteins in hESC-PP, CO PP/hFP-MC, and CO PP/BM-MSC cultures. Scale bar: 50 μm. c) Relative gene expression (2^-Δct) analysis for PP (PDX1 and NKX6-1), endocrine progenitor (NGN3), endocrine (INSULIN and GLUCAGON), and mesenchymal (DESMIN) markers in CO PP/hFP-MC, CO PP/BM-MSC, hESC-PP, and hFP-MC groups. n= 3 biological replicates, each 2 technical repeats. CO PP/hFP-MC, hESC-PP co-cultured with human fetal pancreatic mesenchymal cell; CO PP/BM-MSC, hESC-PP co-cultured with bone marrow mesenchymal stem cell; hESC-PP, human embryonic stem cell-derived pancreatic progenitor cultured solely in 3D system; and hFP-MC, human fetal pancreatic mesenchymal cell cultured solely in 3D system. All error bars represent SEM. Asterisks represent significant differences (* $P < 0.05$ and ** $P < 0.01$).

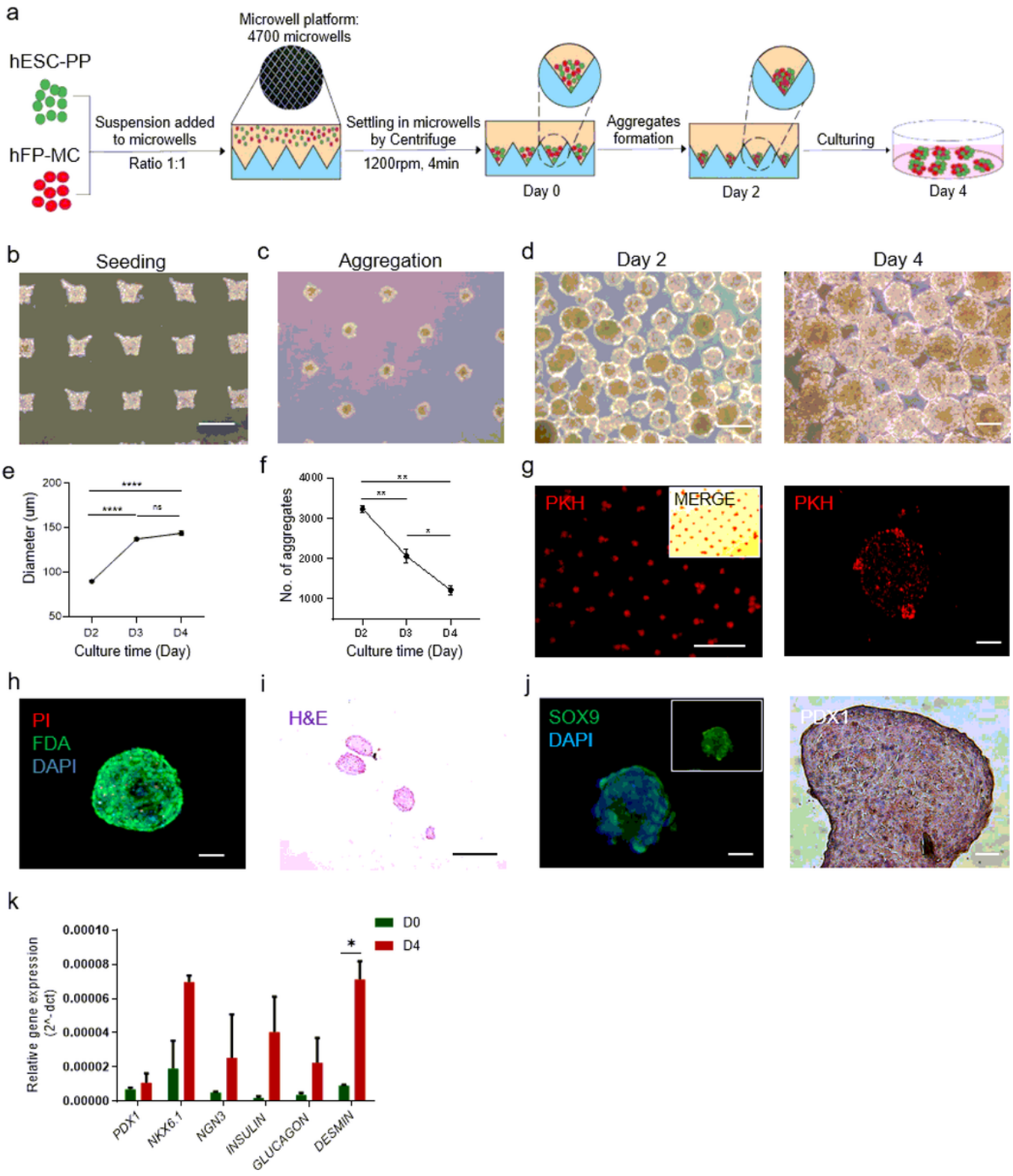

Figure 5

Generation of dual cell-pancreatic aggregates (DC-PA) through 3D microwell system a) A schematic presentation of DC-PAs production method from the combination of hESC-PPs and hFP-MCs in non-adherent microwell platform (containing 4700 microwells) and further culture in static suspension condition for 4 days. b) Phase-contrast image of hESC-PP and hFP-MC cells (1:1 ratio at the final concentration of 500 cells/microwell) settled into microwells after centrifuge. Scale bar: 200 µm. c)

Phase-contrast images of DC-PAs formed after 48 hours in microwells. d) Bright-field images of DC-PAs after 2 and 4 days in culture. Scale bars: left: 200 μm; right 100 μm. e) Quantification of the DC-PAs average diameter in suspension culture at three different time-points. Asterisks represent significant differences between groups (P <0.000, ns: non-significant, P ≥ 0.05. N=3 biological replicates). f) Quantification of the average number of DC-PAs at three different time-points. Asterisks represent significant differences between groups (P <0.001 and P <0.01). g) PKH26-labeled hFP-MCs in DC-PAs after 24 hours in microwell chip and after 4 days in culture. Scale bar: 500 μm and 50 μm (left and right images, respectively). h) Confocal image of live/dead staining for DC-PAs on day 4 in culture (maximal projection of 150 μm-thick Z stack). Scale bar: 50 μm. i) Hematoxylin and eosin (H&E) staining of DC-PAs on day 4 of culture. Scale bar: 200 μm. j) Immunostaining for SOX9 marker in DC-PAs on day 4 of culture. Scale bar: 50 μm. k) Relative expression (2^-Δct) of different genes in DC-PAs. N=2 biological replicates. All error bars represent SEM.

Supplementary Files

This is a list of supplementary files associated with this preprint. Click to download.

- graphicalabstract.jpeg
- Supplementaryforcellularmolecularlifesciences.pdf